Effect of Fault Severities and Noise Levels on Fault Isolation in 7-Phase Electrical Machines

Lu Zhang, Claude Delpha, Demba Diallo

Effect of Fault Severities and Noise Levels on Fault Isolation in 7-Phase Electrical Machines

Lu ZHANG*, Claude DELPHA*, Demba DIALLO†

*Université Paris Saclay, CNRS, CentraleSupélec, Laboratoire des Signaux et Systèmes - Gif sur Yvette, France
†Université Paris Saclay, CentraleSupélec, CNRS, Group of Electrical Engineering of Paris - Gif sur Yvette, France

IECON 2023- 49th Annual Conference of the IEEE Industrial Electronics Society | 979-8-3503-3182-0/23/$31.00 ©2023 IEEE | DOI: 10.1109/IECON51785.2023.10312583

***Abstract*—This paper presents a fast and efficient fault isolation method in 7-phase electrical machines based on the phase currents projections in the stationary reference frames. The study considers both non incipient faults with 15% to 30% fault severities, and incipient ones whose severities vary 1% to 6%. The noise level effect on the fault isolation is also considered. The fault features are extracted from the transformed currents in the frequency domain. The features are processed with a multi-step classification methodology based on usual techniques (principal component analysis, linear discriminant analysis and support vector machine). The simulation results show that the fault classification under low noise level conditions is effective with an accuracy higher than 98%. However, when the noise level increases, the proposal fails to classify incipient faults.**

***Index Terms*—Fault isolation, Stationary frame, Non-incipient faults, Incipient faults, Noise levels**

I. Introduction

Fault Detection and Diagnosis (FDD) can be decomposed in three steps: detection (detect if a change has occurred), isolation (isolate the fault location and type), and estimation (estimate the fault severity) [1].

Once the fault is detected, it can be isolated and its severity estimated. Indeed, in a complex system the faults can affect any component (electrical machine, energy storage systems, cables, connectors, ...) [2]. The fault type identification and its location are important steps for an accurate fault estimation that is crucial for maintenance and reliability purposes. Therefore, this work will mainly focus on the isolation process. Undoubtedly, the wide range of fault types is a significant challenge to fault isolation [3]. In recent years, advanced machine learning techniques, such as deep learning and reinforcement learning, are actively investigated to improve fault isolation performance [4]–[8]. For example, in [4], the authors proposed applying a Back-Propagation (BP) neural network architecture as an alternative method for fault detection, classification, and isolation in a transmission line system. In [5], the authors presented a novel fault classification method for high-speed relay protection systems based on multiple neural networks. Besides, there is a growing trend to combine the advantages of model-based and data-driven approaches for fault isolation, especially for non-linear systems [9]–[12]. In [11], the authors proposed a combined approach that integrated Cuckoo Search Optimization (CSO) and Relevance Vector Machine (RVM) to classify open and short-circuit faults in three-phase inverter, which aimed to achieve higher fault classification accuracy while minimizing the training and testing durations. Reference [12] proposed a method for classifying any-phase or multi-phase faults on transmission lines using Radial Basis Function Neural Network (RBFNN) and Recursive Least Squares (RLS) algorithm. Although these advanced machine learning methods can handle complex high-dimensional data, they usually require huge amount of training data to achieve optimal performance. If not, the learned models may be biased or inaccurate. Additionally, preparing and collecting large, high-quality datasets can be time- and resource-intensive. Therefore, the approach proposed in this paper relies only on fault features in the frequency domain and simple and popular approaches to isolate fault types, as the follow-up in [13].

The authors would like to thank China Scholarship Council.

In [13], the authors developed an analytical model of the phase currents in a 7-phase machine, with a focus on the transformed components in the stationary reference frames. This model assumed that most of the faults in the electrical drive affect the parameters (amplitude, bias and phase shift) of the phase currents. It was shown that the transformed currents in the fictitious four machines are effective fault features with significant fault signatures in the frequency domain. The DC and fundamental components are of particular interest. Consequently, the proposed fault classification method is based on these features. The performance of the classification will be analysed for non incipient and incipient faults with different fault severities, and under varying noise levels.

The contributions of this paper are: (1) Proposal of fault isolation features: the amplitude of $0F$ and $1F$ components of the transformed phase currents. (2) Fault isolation analysis for non incipient and incipient fault types with different fault severities. (3) Fault isolation performance under different noise levels.

The paper is organized as follows: Section II briefly introduces the analytical model and the dataset. Section III presents several classification approaches. Section IV discusses different scenarios (non incipient and incipient faults under different noise levels). The conclusion and perspectives are given in Section V.

II. Data description

The phase currents in 7-phase machines can be modelled in the natural, stationary (α, β), or synchronous (d, q) frame. The stationary and synchronous frames are based on a decomposition of the actual machine into four fictitious machines: a one-phase Homopolar Machine (HM) and three independent and orthogonal coordinate fictitious machines: Principal Machine (PM), Secondary Machine (SM), and Tertiary Machine (TM), in $\alpha-\beta$ planes or $d-q$ planes [13]. In the following, only the (α, β) reference frame is considered due to space limitation.

The faulty currents in the natural frame can be expressed in (1). It is assumed that that no matter the fault type and evolution, the fault effect on the phase currents can be emulated with three parameters ($\triangle i_j$, ϕ_j and γ_j). The faulty currents, projected into the stationary frame with the Clarke transformation, are expressed in (2).

$$i_{j(j=1\ldots7)f} = I\sqrt{2}(1+\triangle i_j)sin(\theta+(1-j)\varphi+\phi_j)+\gamma_j \quad (1)$$

where, $\theta = \omega t$, ω is the angular frequency, t is the current time, φ is the natural phase shift equal to $\frac{2\pi}{7}$ in 7-phase machine, I is the RMS value of the phase current. $\triangle i_j$, ϕ_j and γ_j will represent the fault parameters resulting in a modification of the amplitude, initial phase shift, and bias, respectively.

Fault frequencies in the stationary frame are summarized in TABLE I. The spectrum of the faulty current in the stationary frame includes DC ($0F$) and/or fundamental component ($1F$).

TABLE I: Fault frequencies in the stationary frame

Case	Current		Harmonic		Case	Current		Harmonic	
			$0F$	$1F$				$0F$	$1F$
H	PM	$i_{p\alpha}$		×	G	PM	$i_{p\alpha}$		×
		$i_{p\beta}$		×			$i_{p\beta}$		×
	SM	$i_{s\alpha}$				SM	$i_{s\alpha}$		×
		$i_{s\beta}$					$i_{s\beta}$		$\times^{(1)}$
	TM	$i_{t\alpha}$				TM	$i_{t\alpha}$		×
		$i_{t\beta}$					$i_{t\beta}$		$\times^{(1)}$
	HM	i_0				HM	i_0		×
PS	PM	$i_{p\alpha}$		×	MV	PM	$i_{p\alpha}$	×	×
		$i_{p\beta}$		×			$i_{p\beta}$	$\times^{(2)}$	×
	SM	$i_{s\alpha}$		×		SM	$i_{s\alpha}$	×	
		$i_{s\beta}$		$\times^{(1)}$			$i_{s\beta}$	$\times^{(3)}$	
	TM	$i_{t\alpha}$		×		TM	$i_{t\alpha}$	×	
		$i_{t\beta}$		$\times^{(1)}$			$i_{t\beta}$	$\times^{(3)}$	
	HM	i_0		×		HM	i_0	×	

H: healthy conditions; G: gain fault; PS: phase shift fault; MV: mean value fault.
(1) For phase 1, no $1F$ component for $i_{s\beta}$ and $i_{t\beta}$.
(2) For phase 1, no $0F$ component for $i_{p\beta}$.
(3) For phase 1, no $0F$ component for $i_{s\beta}$ and $i_{t\beta}$.

The amplitudes of the transformed currents in the stationary frame will be used as features to isolate the faults. The dataset (TABLE II) is composed of:

- Three fault types: gain fault (g), phase shift fault (ps) and mean value fault (mv).
- Several fault severities: incipient faults [1% to 6%] and non incipient faults [15% to 30%].
- Different noise levels: 20 dB and 5 dB. The noise level is defined by considering the Signal to Noise Ratio (SNR), $SNR = 10 \times \log_{10}\frac{\sigma_s^2}{\sigma_\upsilon^2}$, where, σ_s^2 is the variance of the signal, and σ_υ^2 the variance of the Gaussian distributed noise, $\upsilon \sim \mathcal{N}(0, \sigma_\upsilon^2)$.

There are two components ($0F$ and $1F$) for the seven currents in total, under study. Thus the data matrix $\widetilde{\boldsymbol{Y}}_{[N\times M]}$ is expressed in (3), where, N is the number of samples, and M the number of variables equal to 14. In the following, the fault classification will be evaluated for both fault types (non incipient and incipient) with different fault severities and noise levels.

III. Isolation techniques

For this application, linear (Principal Component Analysis, Linear Discriminant Analysis), and non linear techniques (Support Vector Machine) are investigated. Indeed, these techniques are very popular and already successfully used in several applications.

A. Principal Component Analysis (PCA)

Principal Component Analysis, an unsupervised method, initially proposed by Pearson (1901) and later developed by Hotelling (1947), is a standard multivariate technique. Its main advantage is its ability to identify the underlying structure or patterns in high-dimensional data through a projection into a lower-dimensional space, while keeping the maximum information variance [14].

The PCA is done in the following steps:

1) Normalize the data to have zero mean and unit variance:

$$\begin{aligned}\overline{\widetilde{\boldsymbol{Y}}}_{[N\times M]} &= [\overline{\widetilde{\boldsymbol{y}}}_{p\alpha(0F)}, \cdots, \overline{\widetilde{\boldsymbol{y}}}_{0(0F)}, \overline{\widetilde{\boldsymbol{y}}}_{p\alpha(1F)}, \cdots, \overline{\widetilde{\boldsymbol{y}}}_{0(1F)}] \\ &= \begin{bmatrix} \overline{\widetilde{y}}_{1-p\alpha(0F)} & \cdots & \overline{\widetilde{y}}_{1-p\alpha(1F)} & \cdots \\ \vdots & \vdots & \vdots & \vdots \\ \overline{\widetilde{y}}_{i-p\alpha(0F)} & \cdots & \overline{\widetilde{y}}_{i-p\alpha(1F)} & \cdots \\ \vdots & \vdots & \vdots & \vdots \\ \overline{\widetilde{y}}_{N-p\alpha(0F)} & \cdots & \overline{\widetilde{y}}_{N-p\alpha(1F)} & \cdots \end{bmatrix}\end{aligned} \quad (4)$$

where, N is the number of samples, $i \in [1, N]$, and M the number of variables equal to 14.

2) Compute the covariance matrix $\mathbf{C}_{[M\times M]}$.
3) Compute the eigenvectors ($\mathbf{P}_{[M\times M]}$) and eigenvalues ($\Lambda_{[M\times M]}$) of the covariance matrix $\mathbf{C}_{[M\times M]}$. The eigenvectors represent the principal components, while the eigenvalues show the explained variance of each component.

$$\mathbf{CP} = \Lambda\mathbf{P} \quad (5)$$

$$\Lambda = \begin{bmatrix} \lambda_1 & & & & \\ & \ddots & & & \\ & & \lambda_j & & \\ & & & \ddots & \\ & & & & \lambda_M \end{bmatrix} \quad (6)$$

$$\mathbf{P} = [\mathbf{p}_1 \quad \cdots \quad \mathbf{p}_j \quad \cdots \quad \mathbf{p}_M] \quad (7)$$

$$\begin{pmatrix} i_0 \\ i_{p\alpha} \\ i_{p\beta} \\ i_{t\alpha} \\ i_{t\beta} \\ i_{s\alpha} \\ i_{s\beta} \end{pmatrix} = \sqrt{\frac{2}{7}} \begin{pmatrix} \frac{1}{\sqrt{2}} & \frac{1}{\sqrt{2}} & \frac{1}{\sqrt{2}} & \frac{1}{\sqrt{2}} & \frac{1}{\sqrt{2}} & \frac{1}{\sqrt{2}} & \frac{1}{\sqrt{2}} \\ 1 & cos(\varphi) & cos(2\varphi) & cos(3\varphi) & cos(4\varphi) & cos(5\varphi) & cos(6\varphi) \\ 0 & sin(\varphi) & sin(2\varphi) & sin(3\varphi) & sin(4\varphi) & sin(5\varphi) & sin(6\varphi) \\ 1 & cos(2\varphi) & cos(4\varphi) & cos(6\varphi) & cos(8\varphi) & cos(10\varphi) & cos(12\varphi) \\ 0 & sin(2\varphi) & sin(4\varphi) & sin(6\varphi) & sin(8\varphi) & sin(10\varphi) & sin(12\varphi) \\ 1 & cos(3\varphi) & cos(6\varphi) & cos(9\varphi) & cos(12\varphi) & cos(15\varphi) & cos(18\varphi) \\ 0 & sin(3\varphi) & sin(6\varphi) & sin(9\varphi) & sin(12\varphi) & sin(15\varphi) & sin(18\varphi) \end{pmatrix} \begin{pmatrix} i_1 \\ i_2 \\ i_3 \\ i_4 \\ i_5 \\ i_6 \\ i_7 \end{pmatrix} \tag{2}$$

TABLE II: Number of samples in the simulations

SNR (dB)	Fault types	Number of samples									
		incipient faults						non incipient faults			
		1%	2%	3%	4%	5%	6%	15%	20%	25%	30%
20	g	200	200	200	200	200	200	200	200	200	200
	ps	200	200	200	200	200	200	200	200	200	200
	mv	200	200	200	200	200	200	200	200	200	200
5	g	200	200	200	200	200	200	200	200	200	200
	ps	200	200	200	200	200	200	200	200	200	200
	mv	200	200	200	200	200	200	200	200	200	200

g: gain fault; ps: phase shift fault; mv: mean value fault.

$$\begin{aligned} \widetilde{\boldsymbol{Y}}_{[N\times M]} = [&\widetilde{\boldsymbol{y}}_{p\alpha(0F)}, \widetilde{\boldsymbol{y}}_{p\beta(0F)}, \widetilde{\boldsymbol{y}}_{s\alpha(0F)}, \widetilde{\boldsymbol{y}}_{s\beta(0F)}, \widetilde{\boldsymbol{y}}_{t\alpha(0F)}, \widetilde{\boldsymbol{y}}_{t\beta(0F)}, \widetilde{\boldsymbol{y}}_{0(0F)}, \\ &\widetilde{\boldsymbol{y}}_{p\alpha(1F)}, \widetilde{\boldsymbol{y}}_{p\beta(1F)}, \widetilde{\boldsymbol{y}}_{s\alpha(1F)}, \widetilde{\boldsymbol{y}}_{s\beta(1F)}, \widetilde{\boldsymbol{y}}_{t\alpha(1F)}, \widetilde{\boldsymbol{y}}_{t\beta(1F)}, \widetilde{\boldsymbol{y}}_{0(1F)}] \end{aligned} \tag{3}$$

4) Sort the eigenvalues in descending order to determine the eigenvectors that span the principal and residual subspaces. Typically, the principal subspace is spanned with the eigenvectors whose Cumulative Percent of Variance (CPV) is higher than 95%.

$$\texttt{CPV}(l) = \frac{\sum_{j=1}^{l} \lambda_j}{\sum_{j=1}^{M} \lambda_j} \geq 95\% \tag{8}$$

5) Create the projection matrix whose columns are the eigenvectors. This matrix will be used to project the actual data into lower-dimensional subspaces (principal or residual).

$$\widetilde{\widetilde{\boldsymbol{Y}}}_{[N\times l]} = \overline{\widetilde{\boldsymbol{Y}}}_{[N\times M]} \mathbf{P}_{[M\times l]} \tag{9}$$

B. Linear Discriminant Analysis (LDA)

Linear Discriminant Analysis is a supervised machine learning algorithm that can discriminate classes that can be linearly separated. It is based on the simultaneous maximisation of inter-class and minimization intra-class variances [15]. The key point is the computation of the inter-class matrix $\boldsymbol{S_b}$ and intra-class matrix $\boldsymbol{S_w}$ from which the eigenvalues and eigenvectors of the matrix ${\boldsymbol{S_w}}^{-1}\boldsymbol{S_b}$ can be obtained.

$$\boldsymbol{S_b} = \sum_{k=1}^{p} N_k(\mu_k - \mu)(\mu_k - \mu)^T \tag{10}$$

$$\boldsymbol{S_w} = \sum_{k=1}^{p} \sum_{\widetilde{y}\in\widetilde{\boldsymbol{Y}}_k} (\widetilde{y} - \mu_k)(\widetilde{y} - \mu_k)^T \tag{11}$$

where, $N_k(k = 1, 2, \cdots, p)$ is the number of the k_{th} class, $\widetilde{\boldsymbol{Y}}_k(k = 1, 2, \cdots, p)$ is the set of the k_{th} class, $\mu_k(k = 1, 2, \cdots, p)$ is the mean value of the k_{th} class, μ is the mean value of the whole samples.

LDA exhibits higher classification performance than PCA when the main change between the sampled data affect the average values. LDA and PCA are optimal when the data follow a Gaussian distribution, which is the case in this study as shown in [16]. Therefore, they can be used in the following.

C. Support Vector Machine (SVM)

Support Vector Machine is a supervised machine learning algorithm that can handle the separation of classes, which are linearly or non-linearly separable. The main idea behind SVM is to find an optimal hyperplane that best separates the data points of different classes in the feature space. In non-linear cases, the key is to choose an appropriate kernel function to map the input features into a higher dimensional space. Common kernel functions include linear, polynomial, Radial Basis Function (RBF), and sigmoid [17].

IV. Numerical simulations

In the following simulations, we consider three single non incipient faults [15% to 30%] and three single incipient faults

[1% to 6%] under different noise levels (20 dB and 5 dB), to evaluate the classification performance.

A. Low noise level case

In this section, the noise level is considered as low with a SNR set to 20 dB. First, the data matrix $\widetilde{\boldsymbol{Y}}$ is analyzed using PCA. The results are depicted in Fig. 1. From the initial fourteen variables, we can observe that the cumulative sum of the first three principal components exceeds 95% (Fig. 1-a). However, if the data is projected in the subspace defined by the first two principal components (representing almost 90% of the initial total information), the two classes (non incipient and incipient faults) can be linearly separated (Fig. 1-b). Therefore, LDA can be used for fault isolation.

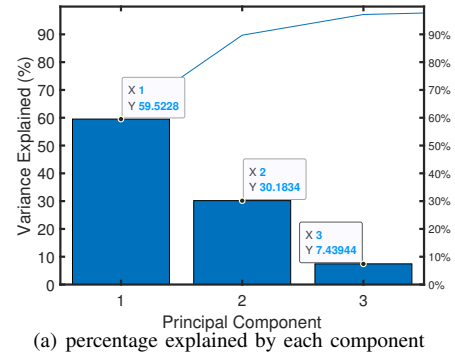

(a) percentage explained by each component

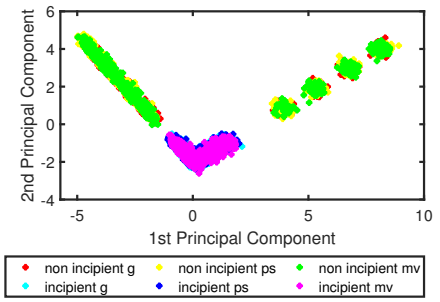

(b) 1st - 2nd PCA representation

Fig. 1: PCA results wtith SNR = 20 dB

The LDA classification results are presented in (Fig. 2). It can be observed that after the first processing the non incipient faults are clearly separated. However, a second step is necessary to separate the data for incipient faults as displayed in (Fig. 3). But, there is still an overlap between the incipient gain fault and incipient phase shift fault. These two classes will be separated with SVM. The presented results are obtained with the following variables: $\widetilde{\boldsymbol{y}}_{0F}$ and $\widetilde{\boldsymbol{y}}_{1F}$ of $i_{p\alpha}$. The classification is evaluated successfully with other variables. A linear kernel is utilized. The results are illustrated in Fig. 4. It can be observed that the separation is highly satisfactory, with an accuracy higher than 98.8%, as displayed in the confusion matrix presented in (12). It can be concluded that when the measurement noise level is low, non incipient and incipient faults can be clearly separated with a linear classifier in a lower dimension feature space. However, in the case of incipient faults, a higher dimension is required with a linear SVM to handle the overlap between gain and phase shift faults. Finally, the flowchart of the classification is shown in Fig. 5.

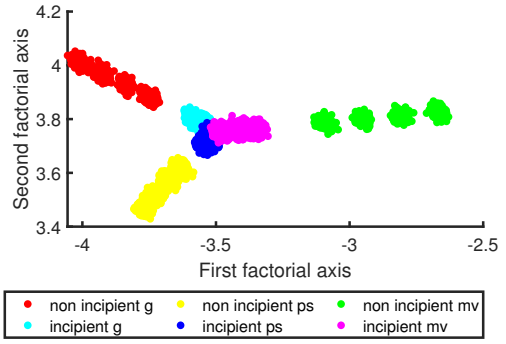

Fig. 2: Step 1: LDA classification when SNR = 20 dB

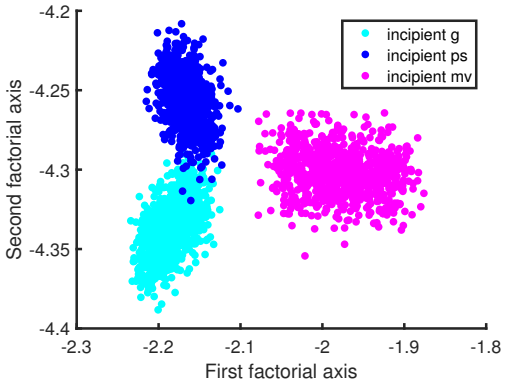

Fig. 3: Step 2: LDA classification when SNR = 20 dB

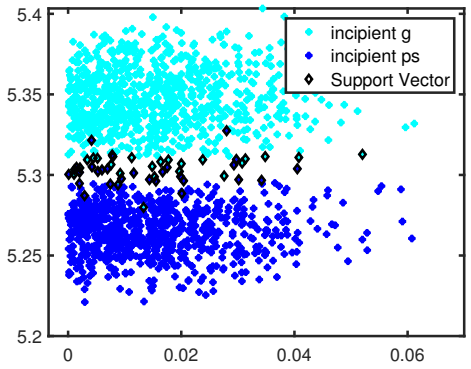

Fig. 4: Step 3: Linear SVM classification when SNR = 20 dB

$$\texttt{confusion matrix} = \begin{bmatrix} 98.9\% & 1.1\% \\ 1.2\% & 98.8\% \end{bmatrix} \tag{12}$$

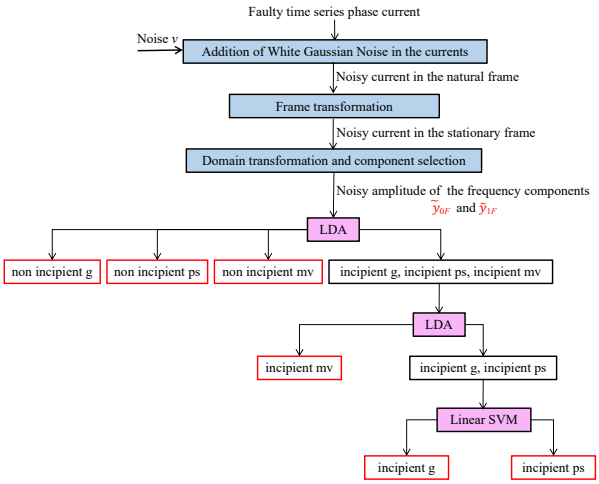

Fig. 5: Fault isolation flowchart with SNR = 20 dB

B. High noise level case

In this section, we assume that the phase current measurements are highly corrupted with the noise, with SNR set to 5dB. The PCA results are presented in Fig. 6. Fig. 6-b shows significant overlaps in the 2D frame spanned by the first two principal components. This is confirmed by the cumulative sum percentage displayed in Figure 6-a from which it can be observed that PCA will not be effective in this case. One can only expect a separation of the non incipient and incipient classes.

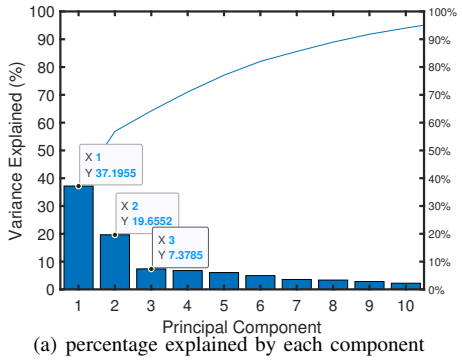

(a) percentage explained by each component

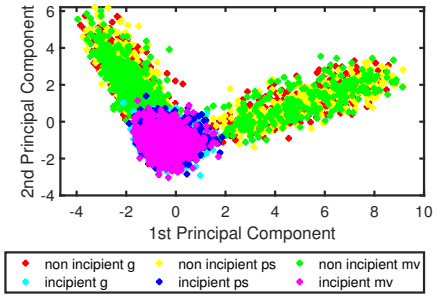

(b) 1st - 2nd PCA representation

Fig. 6: PCA results with SNR = 5 dB

The LDA results are displayed in Fig. 7. One can observe an improvement because the non incipient mean value fault can now be discriminated from all the other ones.

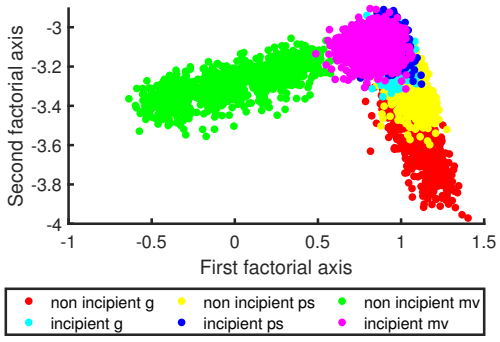

Fig. 7: Step 1: LDA classification when SNR = 5 dB

Then, LDA is performed on the data matrix from which the mean value fault data are removed. The results are shown in Fig. 8, and the confusion matrix, in (13). There is a significant improvement as the remaining non incipient faults can be separated.

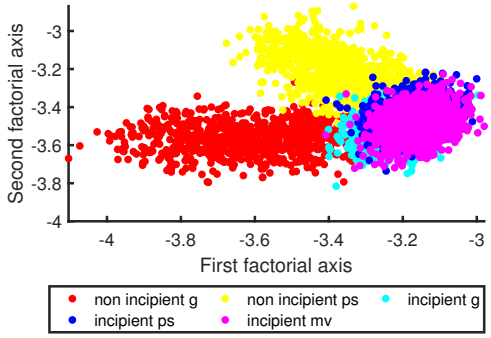

Fig. 8: Step 2: LDA classification results with SNR = 5 dB

$$\texttt{confusion matrix} = \begin{bmatrix} 95.2\% & 4.8\% \\ 2.8\% & 97.2\% \end{bmatrix} \quad (13)$$

The classification of non incipient gain and phase shift faults can be improved with a linear SVM classifier as shown in Fig. 9, and the confusion matrix in (14). Non incipient gain and phase shift faults can be separated with an accuracy higher than 98.5%.

$$\texttt{confusion matrix} = \begin{bmatrix} 98.6\% & 1.4\% \\ 1.5\% & 98.5\% \end{bmatrix} \quad (14)$$

From the previous results, it can be concluded that PCA, LDA and even SVM with a non linear kernel failed to classify incipient faults when the phase currents measurements are highly corrupted with noise. Consequently, the classification flowchart under high noise level conditions is depicted in Fig. 10.

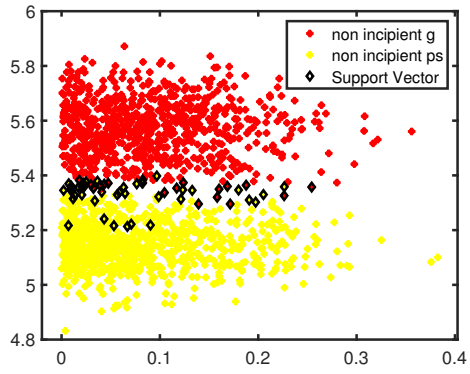

Fig. 9: Step 3: Linear SVM classification results with SNR $= 5$ dB

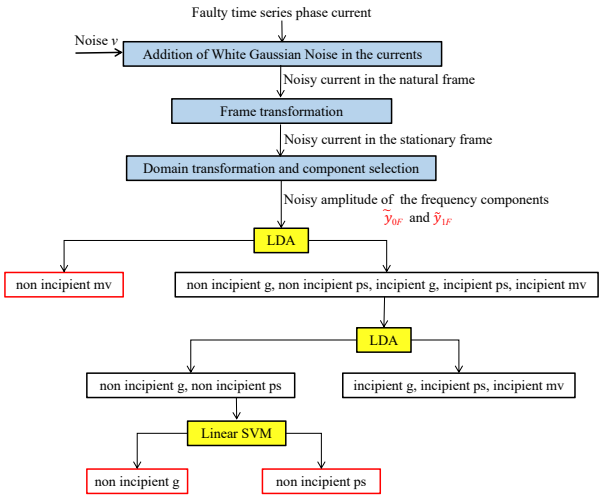

Fig. 10: Fault isolation flowchart with SNR $= 5$ dB

V. Conclusion

This paper proposes a fault classification methodology based on popular simple classifiers (PCA, LDA and SVM) to discriminate faults in 7-phase electrical machines. The proposal is evaluated for different fault severities (non incipient and incipient faults) and under high and low noise levels. The proposal uses the amplitudes of phase currents projected in the Clarke stationary reference frames.

The simulation results show that under low noise level, the multiple-step classification methodology is successful in separating non incipient faults from incipient ones, and also successful in discriminating the fault types. However, when the noise level increases, the proposal is only successful in discriminating non incipient faults from incipient ones, and separating non incipient fault types. Future works will be devoted to find more relevant incipient fault features. Mixed faults could also be considered as they may be representative of faults that may occur with the complex system.

References

[1] J. Gertler, *Fault detection and diagnosis in engineering systems*. CRC press, 1998.

[2] C. M. Furse, M. Kafal, R. Razzaghi, and Y.-J. Shin, "Fault diagnosis for electrical systems and power networks: A review," *IEEE Sensors Journal*, vol. 21, no. 2, pp. 888–906, 2020.

[3] S. Soliman and M. Belkhayat, "Power systems fault type identification based on park's transformation algorithm," in *2006 Large Engineering Systems Conference on Power Engineering*. IEEE, 2006, pp. 141–145.

[4] E. B. M. Tayeb and O. A. A. A. Rhim, "Transmission line faults detection, classification and location using artificial neural network," in *2011 International Conference & Utility Exhibition on Power and Energy Systems: Issues and Prospects for Asia (ICUE)*. IEEE, 2011, pp. 1–5.

[5] T. Dalstein and B. Kulicke, "Neural network approach to fault classification for high speed protective relaying," *IEEE Transactions on Power Delivery*, vol. 10, no. 2, pp. 1002–1011, 1995.

[6] R. Iqbal, T. Maniak, F. Doctor, and C. Karyotis, "Fault detection and isolation in industrial processes using deep learning approaches," *IEEE Transactions on Industrial Informatics*, vol. 15, no. 5, pp. 3077–3084, 2019.

[7] M. Li, H. Zhang, T. Ji, and Q. Wu, "Fault identification in power network based on deep reinforcement learning," *CSEE Journal of Power and Energy Systems*, vol. 8, no. 3, pp. 721–731, 2021.

[8] L. Wen, X. Li, and L. Gao, "A new reinforcement learning based learning rate scheduler for convolutional neural network in fault classification," *IEEE Transactions on Industrial Electronics*, vol. 68, no. 12, pp. 12 890–12 900, 2020.

[9] D. Jung, K. Y. Ng, E. Frisk, and M. Krysander, "Combining model-based diagnosis and data-driven anomaly classifiers for fault isolation," *Control Engineering Practice*, vol. 80, pp. 146–156, 2018.

[10] M. A. Atoui and A. Cohen, "Coupling data-driven and model-based methods to improve fault diagnosis," *Computers in Industry*, vol. 128, p. 103401, 2021.

[11] V. Gomathy and S. Selvaperumal, "Fault detection and classification with optimization techniques for a three-phase single-inverter circuit," *Journal of Power Electronics*, vol. 16, no. 3, pp. 1097–1109, 2016.

[12] S. Samantaray, P. Dash, and G. Panda, "Fault classification and location using hs-transform and radial basis function neural network," *Electric Power Systems Research*, vol. 76, no. 9-10, pp. 897–905, 2006.

[13] L. Zhang, C. Delpha, and D. Diallo, "Current-based analytical model for fault detection and diagnosis in 7-phase machines," in *IECON 2022–48th Annual Conference of the IEEE Industrial Electronics Society*. IEEE, 2022, pp. 1–6.

[14] S. Wold, K. Esbensen, and P. Geladi, "Principal component analysis," *Chemometrics and intelligent laboratory systems*, vol. 2, no. 1-3, pp. 37–52, 1987.

[15] S. Balakrishnama and A. Ganapathiraju, "Linear discriminant analysis-a brief tutorial," *Institute for Signal and information Processing*, vol. 18, no. 1998, pp. 1–8, 1998.

[16] L. Zhang, C. Delpha, and D. Diallo, "Fault severity estimation in 7-phase electrical machines in a noisy environment," in *ISIE 2023–32nd International Symposium on Industrial Electronics*. IEEE, 2023, pp. 1–6.

[17] M. A. Hearst, S. T. Dumais, E. Osuna, J. Platt, and B. Scholkopf, "Support vector machines," *IEEE Intelligent Systems and their applications*, vol. 13, no. 4, pp. 18–28, 1998.